Clemson University
TigerPrints

Publications   Physics and Astronomy

1-1-2012

Measuring the Stellar Accretion Rates of Herbig Ae/Be Stars

Brian Donehew
Clemson University

Sean D. Brittain
Clemson University, sbritt@clemson.edu

Follow this and additional works at: https://tigerprints.clemson.edu/physastro_pubs

Part of the Astrophysics and Astronomy Commons

Recommended Citation

Please use publisher's recommended citation.

MEASURING THE STELLAR ACCRETION RATES OF HERBIG Ae/Be STARS

BRIAN DONEHEW[1] AND SEAN BRITTAIN[1]
Department of Physics and Astronomy, Clemson University, Clemson, SC 29634-0978, USA; briand@clemson.edu, sbritt@clemson.edu

ABSTRACT

The accretion rate of young stars is a fundamental characteristic of these systems. While accretion onto T Tauri stars has been studied extensively, little work has been done on measuring the accretion rate of their intermediate-mass analogs, the Herbig Ae/Be stars. Measuring the stellar accretion rate of Herbig Ae/Bes is not straightforward both because of the dearth of metal absorption lines available for veiling measurements and the intrinsic brightness of Herbig Ae/Be stars at ultraviolet wavelengths where the brightness of the accretion shock peaks. Alternative approaches to measuring the accretion rate of young stars by measuring the luminosity of proxies such as the Br γ emission line have not been calibrated. A promising approach is the measurement of the veiling of the Balmer discontinuity. We present measurements of this veiling as well as the luminosity of Br γ. We show that the relationship between the luminosity of Br γ and the stellar accretion rate for classical T Tauri stars is consistent with Herbig Ae stars but not Herbig Be stars. We discuss the implications of this finding for understanding the interaction of the star and disk for Herbig Ae/Be stars.

Key words: accretion, accretion disks – stars: general

1. INTRODUCTION

Herbig Ae/Be stars (HAeBes) are young stars ranging from spectral class F2 to O9, usually surrounded by a circumstellar disk of gas and dust (e.g., Herbig 1960; Finkenzeller & Mundt 1984; Vieira et al. 2003; Thé et al. 1994; Malfait et al. 1998). The disks around these higher mass analogs to T Tauri stars dissipate on a timescale of ∼5 Myr. Much of the disk material is removed via accretion onto the star. Mass accretion rates are believed to decrease over time and therefore may help to quantify the evolutionary state of disks around HAeBes. The mass accretion rate is also an important parameter for modeling disk structure and dynamics (D'Alessio et al. 1999, 2001), as well as interpreting the emission spectra of the disk atmosphere (Najita et al. 2003). However, the mass accretion rate for HAeBes is difficult to quantify, and the process that mediates mass accretion is still uncertain.

T Tauri stars, on the other hand, have been well studied and shown to accrete magnetospherically (e.g., Bouvier et al. 2007, and references therein). The magnetic field truncates the disk where the ram pressure of the accreting material is balanced by pressure from the stellar magnetic field. At this truncation radius, the accreting material is channeled into funnel flows and ballistically falls onto the stellar surface. The shock of the impact thermalizes in the photosphere, and the accretion areas on the stellar surface are brightly luminous. The accretion luminosity is seen as an UV excess on the spectral energy distribution (SED) of the star (Calvet & Gullbring 1998; Gullbring et al. 2000; Ardila et al. 2002).

It is unclear how much of this picture applies to HAeBes. T Tauri stars are completely convective in their interiors, and it is this convection that is thought to generate the strong magnetic field necessary to truncate the disk (Feigelson & Montmerle 1999). On the other hand, by the time intermediate-mass stars evolve to the point that they are observed to have a spectral type of A or earlier, they are no longer convective (Palla & Stahler

1993). Additionally, the non-detections of a non-thermal radio signature with sensitive 3.6 cm observations of 57 HAeBes indicate that the surface field strength of these sources is ⩽ 10 kG (Skinner et al. 1993).

However, many HAeBes are X-ray emitters, which suggests that HAeBes may possess chromospheres or cornaes, and thus be magnetically active (Skinner & Yamauchi 1996; Stelzer et al. 2006). It is possible that such fields are generated by the differential rotation of HAeBes (Tout & Pringle 1995) or that the magnetic field originates in dynamos within the circumstellar disk (Tout & Pringle 1996). On the other hand, the X-rays may originate from an undetected low mass companion star. Unfortunately, it is difficult to directly measure the magnetic field of HAeBes.

HAeBes are fast rotators, so rotational broadening masks any Zeeman broadening of the spectral lines. Magnetic fields also polarize light, but the field must have a strong longitudinal component to be detectable. Further, it is possible that the polarization cancels, so circular polarization measurements are not sensitive to the overall strength of the magnetic field (e.g., Valenti & Johns-Krull 2004). As with T Tauri stars, measurements show minimal polarization in the light from most HAeBes (Hubrig et al. 2007; Wade et al. 2007), though Alecian et al. (2007) found that about 7% of HAeBes have significant (∼1 kG) longitudinal fields. Coincidentally, main-sequence A and B stars that have strong measurable magnetic fields (the Ap/Bp stars) constitute about 5%–10% of A and B stars. This led Alecian et al. (2007) to conclude that the "magnetic" HAeBes are the precursors of the Ap/Bp stars and the magnetic fields of both types of stars is a fossil relic left over from the initial cloud collapse that formed the star.

Since it is expected that most HAeBes have weak global magnetic fields, one might conclude that they do not accrete magnetospherically. However, there is circumstantial evidence to the contrary. For example, many line profiles show a high velocity redshifted absorption component, indicative of infalling material with supersonic velocity (Muzerolle et al. 2004; Natta et al. 2000; Grinin et al. 2001). Brittain et al. (2009) summarize several lines of evidence that the HBe star HD 100546 is accreting magnetospherically. For example, the Balmer emission

---

[1] Visiting Astronomer, Kitt Peak National Observatory, National Optical Astronomy Observatory, which is operated by the Association of Universities for Research in Astronomy (AURA) under cooperative agreement with the National Science Foundation.

lines reveal red-shifted absorption components (Guimarães et al. 2006) and highly ionized species such as O VI have maximum velocities of ∼600 km s^{-1} (Deleuil et al. 2004).

For classical T Tauri stars (CTTSs), the excess luminosity from mass accretion is often measured in the blue and near ultraviolet (NUV) bands and then used to calculate the mass accretion rate (Valenti et al. 1993; Gullbring et al. 1998). HAeBes peak in brightness in the same wavelength regions as the accretion luminosity, and the accretion luminosity of HAeBes is often of the same scale as the uncertainties in the photospheric luminosity of the star due to uncertainties in distance, spectral type, and extinction (Muzerolle et al. 2004). Thus the separation of the accretion luminosity from the photospheric luminosity is difficult rendering this method unusable for measuring the stellar accretion rate of HAeBes.

The accretion process gives rise to many emission lines. In particular, the Br γ emission line is thought to originate in the funnel flow (Muzerolle et al. 2001). Indeed, Muzerolle et al. (1998, hereafter MHC98) discovered a tight correlation between the luminosity of the Br γ line and the accretion luminosity. Calvet et al. (2004, hereafter C04) extended this relationship to intermediate-mass T Tauri stars (IMTTSs; 1.5–4 $M_\odot$), the evolutionary predecessors of HAeBes. There is also some indication that this relationship may also hold for at least a few HAeBes (van den Ancker 2005), however, there are several reasons to expect that the relationship should not be the same as that for T Tauri stars in general.

First, as mentioned above, it is not clear that HAeBes accrete magnetospherically. If not, then there are no funnel flows from which Br γ emission can originate, so Br γ emission from the inner disk will scale differently with accretion rate. Second, the large rotation velocity of HAeBes relative to T Tauri stars means that the typical corotation radius for an HAeBe is smaller than the typical corotation radius of a T Tauri star. Since funnel flows originate at the corotation radius, even if the Br γ emission does indeed originate in the funnel flow, one might expect that the funnel flows around HAeBes will be systematically smaller (Muzerolle et al. 2004). Thus even if HAeBes accrete magnetospherically, the relationship between the accretion and Br γ luminosities may be systematically offset from that of T Tauri stars. Third, emission from hydrogen recombination in the stellar wind of HBe stars may dilute the signal arising from a purported funnel flow.

Observational studies seeking to determine the origin of Br γ emission from around HAeBes have produced mixed results. Eisner et al. (2009), using interferometry, reports that, for all of the HAeBes in their sample, Br γ emission is from a compact area near the star, which is consistent with magnetospheric accretion. In contrast, Kraus et al. (2008) find that only one out of the five HAeBes they observe is consistent with Br γ emission forming in a funnel flow. Given the uncertainty surrounding any purported relationship between the luminosity of the Br γ emission line and the stellar accretion rate, it is necessary to calibrate this relationship for HAeBes. If the correlation between the accretion luminosity and the luminosity of Br γ emission for HAeBes is the same as CTTSs, that may point to a common accretion mechanism.

An additional method for measuring the stellar accretion rate of HAeBes is the measurement of the veiling of the Balmer discontinuity (Garrison 1978; Muzerolle et al. 2004). The Balmer discontinuity is a prominent feature in the spectrum of A and B stars short-ward of 4000 Å. It is due to the "bunching up" of the Balmer absorption lines resulting in an abrupt decrease

in the stellar flux at those wavelengths. Garrison (1978) noted that the depth of the Balmer discontinuity was shallower for HAeBes than for their main-sequence counterparts. He proposed that the luminosity due to mass accretion veiled the Balmer discontinuity, causing its depth to decrease. For his sample of HAeBes, Garrison (1978) measured the difference in magnitude between 3640 and 4000 Å, which he designated as D_B. He also obtained the expected D_B for model atmospheres of the same spectral types as his sample stars. The difference (ΔD_B) between the accreting star and the model was used to infer the veiling due to mass accretion. Based on Garrison (1978), Muzerolle et al. (2004) calculated the expected Balmer veiling of the HA2e star UX Or for various mass accretion rates, filling fractions, and accretion energy fluxes.

Building on this work, we present spectra of Br γ and the Balmer discontinuity for 33 HAeBes. We use the relationship between the veiling of the Balmer discontinuity and the stellar accretion rate presented by Muzerolle et al. (2004) to measure the accretion rate of the stars in our sample. We then compare the luminosity of the Br γ line to the inferred accretion rate to determine whether the accretion rate and the luminosity of Br γ are correlated. We also compare the stellar accretion rate as a function of mass to that of CTTSs and IMTTSs.

2. OBSERVATIONS AND DATA REDUCTION

We acquired NUV/optical and near-infrared observations of 33 HAeBe stars spanning the spectral range from F2 to B0 (Table 1). We selected sources from Hillenbrand et al. (1992), Malfait et al. (1998), Thé et al. (1994), and Vieira et al. (2003). We chose our targets to give us good coverage of the range of spectral types of HAeBes. The total number of known HAeBes is relatively small, so we selected stars from multiple star formation regions in order to build our sample. Table 1 lists the stellar parameters for our target stars.

2.1. Infrared Spectra

The Br γ spectra were acquired over a period of 18 months with the 2.1 m telescope on Kitt Peak National Observatory, using the Flamingos infrared imager/spectrograph (Figure 1). We used Flamingos in spectrograph mode ($R = 1300$) with the Ks filter, HK grism and the 3 pixel slit oriented in the N–S direction. Due to flexure in the detector, flats were taken at each star location. We took darks for each of our exposure times. The flat-fielded spectra were cleaned of hot pixels using a boxcar filter. Our target stars are relatively bright, with magnitudes brighter than 10 in the Ks band, allowing us to achieve a signal-to-noise ratio of about 25 with relatively short exposure times (10–20 minutes for most targets).

Spectra were taken using an ABBA nod sequence where the A and B positions of the star were separated by 15″. The data were combined by $(A - B - B + A)/2$ in order to remove the sky emission lines and atmospheric thermal background to first order. We defined the location of the A and B beams on the chip and rectified the spectrum in the spatial direction by fitting the centroid of the point spread function with a second degree polynomial. To wavelength calibrate the data, we took a sky spectrum at each star location, and then compared it to a standard OH line spectrum. To create the standard OH line spectrum we convolved an artificial OH line stick spectra with a Gaussian matched to the resolution of our observations.

Table 1
Herbig Ae/Be Stellar Parameters

Star	Spectral Type	Distance (pc)	Ks Magnitude 2MASS	Mass $(M_\odot)$	Radius $(M_\odot)$	log g
(1)	(2)	(3)	(4)	(5)	(6)	(7)
AB Aur	A0	140[c] ± 20	4.23	3.2[c]	2.7[c]	4.4[g]
BF Ori	A5	460[c] ± 100	7.89	1.4[c]	1.3[c]	4.0[h]
CQ Tau	F2[a]	130[e] ± 26	6.17	1.6	1.5	3.5[h]
HD 142666	A8	114[d] ± 20	6.08	2.10[e]	2.92[e]	4.3[j]
HD 144432	A9	200[e] ± 55	5.89	2.6[d]	1.87[d]	3.4[j]
HD 163296	A1	160[c] ± 15	4.78	2.3[e]	2.1[e]	4.1[j]
HD 179218	A0[a]	240[e] ± 52	3.9	4.3[e]	4.96[e]	4.0[j]
HD 244314	A	510[f] ± 100	8.05	1.9	2.0	4.0
HD 244604	A0[a]	510[f] ± 100	7.12	2.2	2.1	4.0
HD 245185	A1[a]	400[b] ± 80	8.02	2.3[b]	1.7[b]	4.0
HD 249879	B8	1000[f] ± 200	9.06	3.8	3.2	4.0
HD 259431	B6	800[b] ± 327	5.73	12.2[b]	6.4[b]	4.2[g]
HD 250550	B9[a]	700[c] ± 140	6.64	4.8[c]	3.5[c]	4.6[g]
HD 278937	A6[a]	300[f] ± 60	6.86	1.8	1.8	4.0
HD 35187	A2[a]	150[f] ± 57	5.91	2.4	2.3	4.0
HD 36112	A5[a]	200[e] ± 47	5.8	2.0[e]	2.3[e]	4.0
HD 36408	B7	342[f] ± 184	6.02	4.1	3.5	4.0
HD 37806	A2[a]	>230[e]	5.4	2.6[e]	2.1[e]	4.0
HD 38120	B	422[f] ± 230	7.16	4.1	5.9	4.0
HD 50138	B9	289[f] ± 67	4.15	3.3	3.0	4.0
HD 53367	B0	1150[c] ± 380	6.12	34.5[c]	17.4[c]	4.0
HK Ori	A4	450[c] ± 100	7.39	2.0[c]	1.7[c]	3.3[g]
Lk Hα 215	B6[a]	800[a] ± 160	7.03	7.0[c]	5.4[c]	3.9[g]
MWC 480	A3[a]	131[d] ± 20	5.51	1.80[d]	1.67[d]	4.0[i]
PX Vul	F3[a]	420[a] ± 100	7.91	2.0	1.9	4.0
UX Ori	A3[a]	460[c] ± 100	7.21	3.3[c]	3.2[c]	4.0[h]
V1686 Cyg	B2[c]	980[a] ± 200	5.48	8.5[c]	7.5[c]	4.0
V346 Ori	A5	400[e] ± 100	8.56	2.5[d]	2.1[d]	4.0[i]
V350 Ori	A1[a]	450[d] ± 100	8.37	2.7	2.5	4.1[i]
V380 Ori	A1[a]	430[e] ± 100	5.95	3.6[c]	2.8[c]	4.0
VV Ser	B6[a]	330[a] ± 50	6.32	3.3[c]	2.4[c]	4.0
XY Per	A2	350[e] ± 147	6.09	3.3[d]	2.6[d]	3.9[i]
Z CMa	B8	1150[e] ± 300	3.77	3.8	3.2	3.7[g]

Notes. For those stars for which we could not find a stellar radius and mass in the literature, we assumed that the star was on the main sequence and estimated its mass and radius based on its spectral type. For HD 244314 and HD 38120, we assumed a spectral type of A5 and B5, respectively. Manoj et al. (2006) list V1686 Cyg as an F9 star, but we use B5 from Hillenbrand et al. (1992) because it fits our spectra better.
[a] Manoj et al. (2006).
[b] Reed (2003).
[c] Hillenbrand et al. (1992).
[d] Blondel & Djie (2006).
[e] van den Ancker et al. (1998).
[f] Vieira et al. (2003).
[g] Strom et al. (1972).
[h] Grinin et al. (2001).
[i] Montesinos et al. (2009).
[j] Guimarães et al. (2006)

2.2. Optical Spectra

Over ten nights, we observed 33 HAeBes with the Goldcam instrument on the 2.1 m telescope on Kitt Peak (Table 2). The instrument was configured with the 09 grating and the $CuSO_4$ filter. This gave coverage from 3200 to 5200 Å and a spectral resolution of 6.7 Å with a dispersion of 2.47 Å per pixel. Each night we took a series of flats, biases, and standard stars. The flats were used to correct pixel to pixel sensitivity variation. The flat-fielded spectra were cleaned of hot pixels using a boxcar filter and then rectified. The standard stars were reduced in the

same way and then used to correct for large scale instrumental sensitivity. The spectral extracts were wavelength calibrated using spectra acquired with the HeNeAr lamp.

3. RESULTS

In general, A and late B stars show the Br γ line in absorption, due to absorption in the stellar photosphere. Our Br γ spectra must be corrected for the photospheric absorption. In addition, our spectra are veiled by blackbody emission from the circumstellar disk. An undetected low mass companion star may also contribute to the veiling. To obtain the equivalent width of the circumstellar Br γ emission, we corrected our observed equivalent widths for both photospheric absorption and disk veiling in the same manner as Garcia Lopez et al. (2006),

$$W_{circ} = W_{observ} - W_{photo}10^{-0.4\Delta m_K}, \qquad (1)$$

where W_{circ} is the equivalent width of the Br γ emission from the circumstellar material, W_{observ} is the observed equivalent width, and W_{photo} is the equivalent width of the Br γ photospheric absorption line of a star of the same spectral type as the HAeBe, taken from Garcia Lopez et al. (2006) and Wallace & Hinkle (1998). However, the spectral type of some of our target stars is uncertain and these are noted in Table 1. The $10^{-0.4\Delta m_K}$ factor corrects W_{photo} for the veiling of the disk (and any possible low mass companion star), where Δm is the difference in magnitude between the observed K magnitude (taken from the Two Micron All Sky Survey; 2MASS), and the expected K magnitude for a star of the same spectral type and at the same distance as the HAeBe star.

The equivalent width of the Br γ line was converted to flux by scaling the normalized continuum to the flux density inferred from the 2MASS K_s measurement. The fluxes were scaled to luminosities using distances culled from the literature and are presented in Table 1. In Table 2, we present the relevant stellar data, equivalent widths, line fluxes, and line luminosities. Our typical uncertainty in the equivalent width was 0.2 Å. Measurements with larger uncertainties are reported in Table 2. In general, the uncertainty in the line luminosity is dominated by the uncertainty in the distance to the star, though for the stars HD 244314, HD 38120, and V1686 Cyg the uncertainty in the spectral type is also significant. For the nearby sources for which reliable *Hipparcos* measurements are available, we took the uncertainty in the distance from the uncertainty in the parallax. For other sources we adopted an uncertainty of 20%.

We normalized the HAeBe spectrum, and a Kurusz–Castelli (KC) model spectrum of the same spectral type and log g, to the flux at 4000 Å. For the log g values of our target stars, we used the literature value if available (Guimarães et al. 2006; Grinin et al. 2001; Montesinos et al. 2009; Strom et al. 1972). Otherwise, we assumed that log $g = 4.0$, which is a typical value for both HAeBes and T Tauri stars (Schiavon et al. 1995; Strom et al. 1972). We then adjusted the HAeBe spectra to match the KC model comparison spectra between 4000 Å and 4600 Å. For both the HAeBe star spectrum and the KC model star spectrum, we found the relative difference in the mean flux between 4000 and 3640 Å. In this way, we get D_B for both the HAeBe and the KC model star. From the difference between the values of D_B, we calculated the difference in magnitude due to veiling, ΔD_B, for each of our HAeBes,

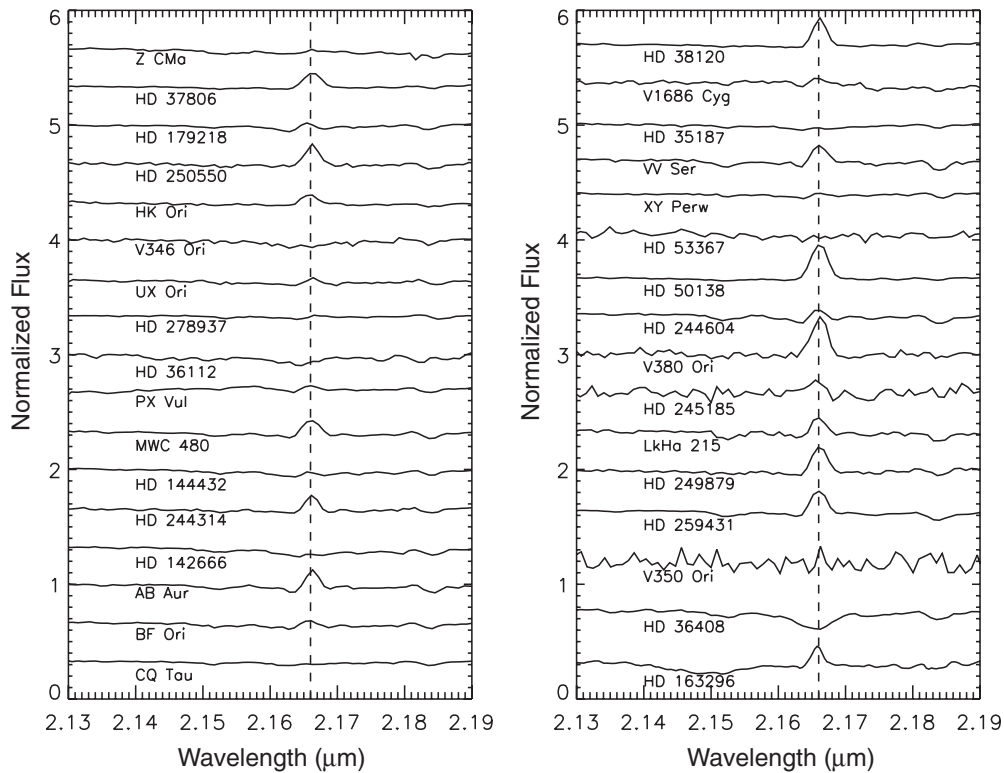$$\Delta D_B = 2.5 \log\left(\frac{F_* + F_A}{F_*}\right), \qquad (2)$$

Figure 1. Spectra of Br γ. The spectra have been normalized and offset for clarity. The dotted vertical line represents the center line of Br γ at 2.166 μm. No emission feature is apparent in some of these sources due to a combination of veiling by the 2 μm continuum of the disk and blending with photospheric absorption.

where F_* is the stellar flux at 3640 Å and F_A is the mass accretion flux at 3640 Å. The typical error for the calculation of ΔD_B is about 0.03 mag. Note that we do not determine, nor do we need to determine, the actual stellar flux or the accretion flux at 3640 Å. We only need the *relative difference* in flux at 3640 Å (see ratio in Equation (2)). We get this by measuring relative difference between the flux at 3640 Å and the normalized flux at 4000 Å for both the HAeBe star and the KC model star spectrum. Figure 2 shows the SEDs of our target stars from 3600 Å to 4400 Å, with SED of the KC model comparison SED overplotted. For many of the HAeBes in the figure, the relative difference in flux at 3640 Å is easily apparent. An important advantage of this technique noted by Muzerolle et al. (2004) is that the measurement of ΔD_B is independent of extinction.

Muzerolle et al. (2004) used the models and methods described in Calvet & Gullbring (1998) and Gullbring et al. (2000) to calculate the flux from accretion and determine the resulting SED, which includes both accretion and stellar photospheric luminosity. We use the results of this model for this work. In this model, mass falls ballistically to the stellar surface along accretion columns, which cover a small fraction (1%–10%) of the surface. The model assumes a plane-parallel flow of material onto the accretion regions of the photosphere. The material has a free-fall velocity when it reaches the photosphere, and carries an energy flux $\mathcal{F}$. The material is traveling at supersonic speed when it reaches the stellar surface, and shocks strongly as it slows down to settle on the surface. The shock region is near the bottom of the photosphere, and the shock region is heated to a temperature $T_S \approx 8.6 \times 10^5 (M_*/0.5\,M_\odot)/(R_*/2\,R_\odot)$ K, releasing soft X-rays that are absorbed by the surrounding material. This material then emits optical and UV radiation as it thermalizes. Muzerolle et al. (2004) calculate the flux from three different regions; the shock region, the heated photosphere, and

the pre-shock accretion column to get the overall flux from accretion. The resulting SEDs, including both the accretion and the photosphere flux, are used to calculate the expected D_B for different mass accretion rates. ΔD_B is then determined by comparison to a standard star of the same spectral type.

We fit a polynomial to the relationship between ΔD_B and the accretion luminosity calculated by Muzerolle et al. (2004). For $\Delta D_B < 0.1$ we adopted an upper limit on the accretion rate of $1.2 \times 10^{-8}\,M_\odot$ yr^{-1}. The accretion luminosity relates to the mass accretion rate via

$$L_{acc} = \frac{GM_* \dot{M}}{R_*}, \qquad (3)$$

where M_* and R_* are the stellar mass and radius, respectively, and $\dot{M}$ is the mass accretion rate. Table 3 shows the results of our Balmer Break measurements. Figure 5 shows accretion luminosity versus Br γ luminosity.

4. ANALYSIS

In Figure 3, we compare the relationship between the luminosity of the Br γ emission line and the accretion luminosity for CTTSs (MHC98), IMTTSs (C04), and HAeBes. From a cursory examination of the data, it appears that the CTTSs, IMTTSs, and HAes follow the same trend while HBes do not. MHC98 showed that the relationship for CTTSs is described by

$$\log(L_{acc}/L_\odot) = (1.26 \pm 0.19)\log(L_{Br\gamma}/L_\odot) + (4.43 \pm 0.79). \qquad (4)$$

In general, most of our targets have higher Br γ and accretion luminosities than the CTTSs. This is mainly a selection effect due to the sensitivity of our measurements. The typical error

Table 2
Herbig Ae/Be Br γ Observations

Star	EW (Obsv.) (Å)	EW (Circ.) (Å)	$F_{\mathrm{Br}\gamma}$ (10^{-14} erg s^{-1} cm^{-2})	$L_{\mathrm{Br}\gamma}$ ($10^{-4} L_\odot$)	Date of Observation
AB Aur	−2.5	−3.9	340 ± 17	21 ± 4	2008 Mar 21
BF Ori	−1.4	−3.6	10.5 ± 0.6	7 ± 2	2006 Nov 11
CQ Tau	± 0.3	−1.1 ± 0.3	16 ± 4	0.83 ± 0.3	2006 Nov 11
HD 142666	1.8	−3.0	47.6 ± 3.2	1.9 ± 0.5	2007 Mar 1
HD 144432	−0.7	−3.0	57 ± 4	7 ± 3	2007 Mar 1
HD 163296	−4.3	−7.1	373 ± 11	30 ± 4	2008 May 13
HD 179218	−1.0	−4.7	80 ± 3	14 ± 4	2007 Sep 23
HD 244314	−2.7	−4.6	12 ± 1	9.6 ± 2.7	2006 Nov 13
HD 244604	−1.8	−2.9	18 ± 1	14 ± 4	2006 Nov 14
HD 245185	−3.8 ± 0.4	−8.2 ± 0.4	22 ± 1	11 ± 3	2006 Nov 11
HD 249879	−5.9	−10.6	11 ± 0	34 ± 10	2006 Nov 15
HD 250550	−4.8	−6.1	58 ± 2	88 ± 25	2006 Nov 12
HD 259431	−5.4	−5.7	125 ± 4	250 ± 140	2006 Nov 14
HD 278937	−0.4	−2.1	16 ± 1	4.5 ± 1	2006 Nov 13
HD 35187	2.0	−2.4	45 ± 4	3 ± 2	2008 Mar 20
HD 36112	−3.7	−5.4	56 ± 4	7 ± 2	2006 Nov 14
HD 36408	7.9	−0.4	7 ± 3	2 ± 2	2006 Nov 15
HD 37806	−3.6	−3.8	112.8 ± 5.9	> 19	2006 Nov 15
HD 38120	−9.2	−9.6	56 ± 1	31 ± 24	2006 Nov 13
HD 50138	−9.2	−9.6	901 ± 19	230 ± 80	2006 Nov 10
HD 53367	± 0.3	−1.7 ± 0.3	26 ± 5	110 ± 50	2007 Mar 1
HK Ori	−3.4	−4.9	23.4 ± 0.9	15 ± 4	2006 Nov 11
LkHα 215	−3.2	−4.4	29 ± 1	58 ± 17	2006 Nov 13
MWC 480	−3.2	−7.0	188 ± 5	10 ± 2	2006 Nov 9
PX Vul	−8.0	−9.6	28.2 ± 0.6	16 ± 5	2007 Sep 23
UX Ori	−0.7	−2.7	15 ± 1	10 ± 3	2008 Mar 22
V1686 Cyg	−1.6	−2.1	58 ± 6	170 ± 50	2007 Sep 24
V346 Ori	1.4	−2.8	4.0 ± 0.3	2.9 ± 0.7	2006 Nov 11
V350 Ori	−1.2 ± 0.6	−7.2 ± 0.3	14 ± 1	9 ± 3	2006 Nov 13
V380 Ori	−9.4	−10.0	179 ± 4	103 ± 34	2006 Nov 15
VV Ser	−3.7	−10.8	137 ± 3	47 ± 10	2007 Sep 24
XY Per	−0.8	−1.8	28 ± 3	10.8 ± 6.5	2006 Nov 9
Z CMa	−0.6	−0.6	80 ± 27	330 ± 160	2007 Mar 3

Note. The typical uncertainty in the equivalent widths for most of our stars is less than 0.2 Å, with the exceptions of V350 Ori and HD 245185, which are given in the table.

for our Br γ equivalent widths (EWs), 0.2 Å, made it difficult to measure Br γ luminosities less than about $10^{-4} L_\odot$. While this can be overcome with more sensitive observations, the more challenging issue is the relationship between the stellar accretion rate and the veiling of the Balmer discontinuity. Measurement of ΔD_B is not sensitive to accretion rates less than $10^{-8} M_\odot$ yr^{-1} (Muzerolle et al. 2004). Following MHC98, we perform a least-squares fit to the data HAes in our sample. We find that

$$\log(L_{\mathrm{acc}}/L_\odot) = (0.9 \pm 0.2)\log(L_{\mathrm{Br}\gamma}/L_\odot) + (3.3 \pm 0.7). \quad (5)$$

The fit to the HAes is remarkably close to the fit to IMTTSs given by C04,

$$\log(L_{\mathrm{acc}}/L_\odot) = 0.9\log(L_{\mathrm{Br}\gamma}/L_\odot) + 2.9. \quad (6)$$

To statistically compare the HAeBes to the CTTSs, we "normalized" both data sets by dividing the measured value of the accretion luminosity by its expected value according to Equation (4). In this way, we get the scatter of both data groups about the expected value. Using the Kolmogrov–Smirnoff test for two samples, we compared the HAes to the CTTSs and determined that there is a 51% probability that both samples are from the same population. Applying the same test to the HBes, we find that there is only a 3% probability that the samples are

drawn from the same population. Thus we conclude that the HAes follow the same trend found for the CTTSs while the HBes do not.

An important concern when looking for a relationship between two luminosities is whether they are truly independent. Since the luminosity is determined by scaling the flux by d^2, it is possible that the d^2 dependency could drive the relationship between the two derived luminosities. The sources presented by MHC98 were all in Taurus, so d^2 dependency of the luminosity is irrelevant for those source, however, the samples of IMTTSs, HAes, and HBes include sources from different distances. To verify that the correlation we observe is not due to the d^2 dependence of the luminosities, we also plot the accretion flux versus the flux of Br γ for the HAeBes, CTTSs (MHC98), and IMTTSs (C04; Figure 4). The relationship between the accretion flux and flux of Br γ is consistent for the CTTSs, IMTTs, and HAes and is given by

$$\log(F_{\mathrm{acc}}/F_\odot) = 1.15 \pm 0.12\log(F_{\mathrm{Br}\gamma}/F_\odot) + 4.61 \pm 0.98. \quad (7)$$

The flux of Br γ emission from HBes continues to overestimate the accretion flux.

There is no particular reason to expect either accretion luminosity or Br γ luminosity to remain constant. If the mass accretion rate of HAeBes varies, then the fact that the Br γ and
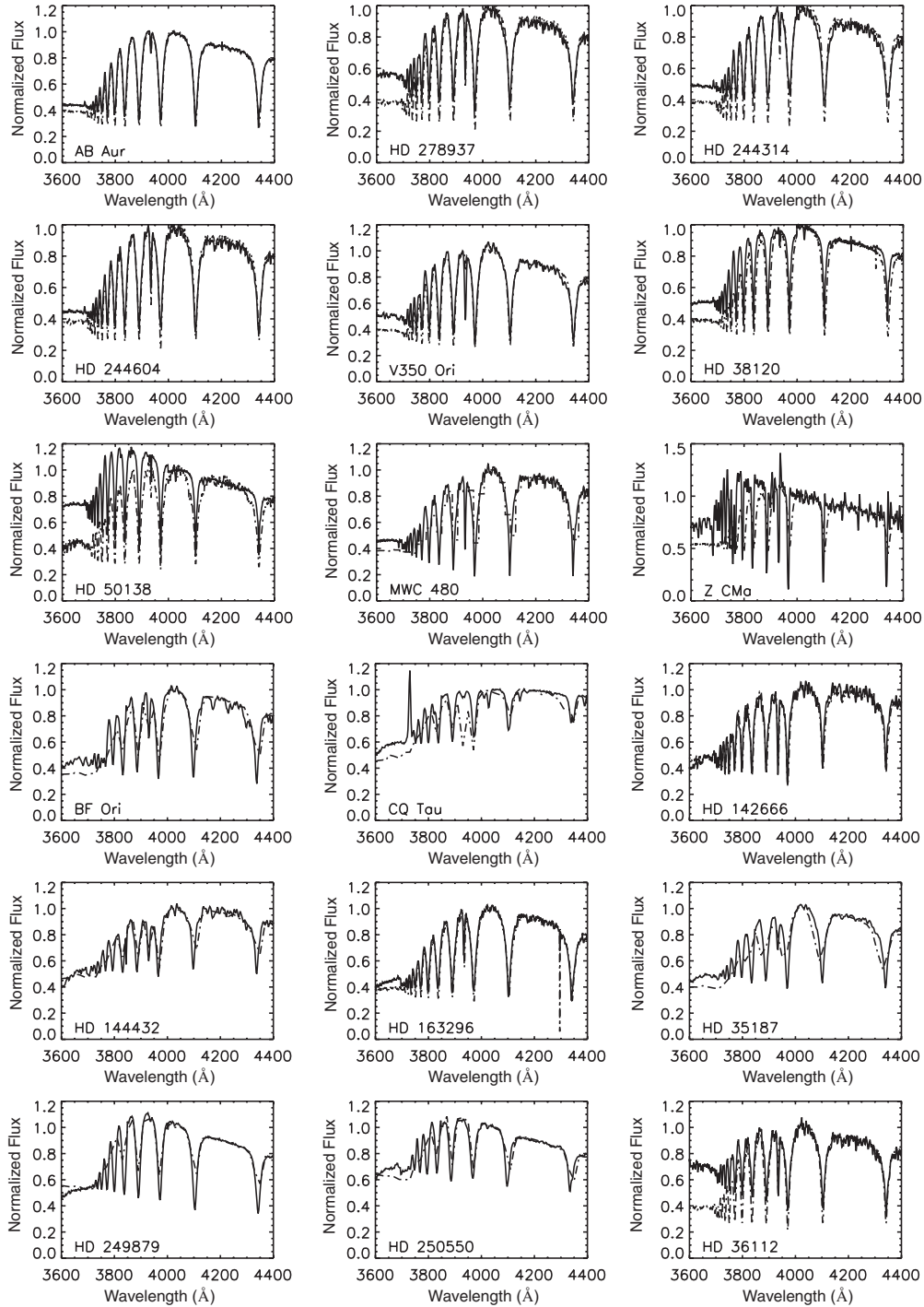
Figure 2. Spectra of the Balmer discontinuity. In each graph, the solid line represents the SED of the HAeBe star. The dashed line represents either the SED of a standard star of the same spectral type or the Kurucz–Castelli model flux for a star of the same spectral type.

Balmer jump spectra were not acquired simultaneously should increase the scatter of the relationship we are searching for. In principle, it is possible that the increase in scatter could be due to an increase in variability with spectral type. To check this, we compare the present multi epoch observations for a subsample of our data.

Table 4 shows the observed equivalent widths for several of our stars taken at different epochs. We also include the observed equivalent widths for these stars (if available) from Garcia Lopez et al. (2006) and Brittain et al. (2007). The variation

of the equivalent widths is less than 1.2 Å for 10 of the 11 stars for which we have two or more observations. This variation is similar in size to the typical uncertainty in the measurement of our equivalent width (< 0.5 Å in most cases). The one exception is HD 36112, where the equivalent width changed by 2.7 Å over 18 months. For some stars the equivalent widths as measured by Garcia Lopez et al. (2006) and Brittain et al. (2007) differ from our values by up to 4 Å. Since the observations of Garcia Lopez et al. (2006) and Brittain et al. (2007) are several years before ours, these differences may reflect genuine variability.
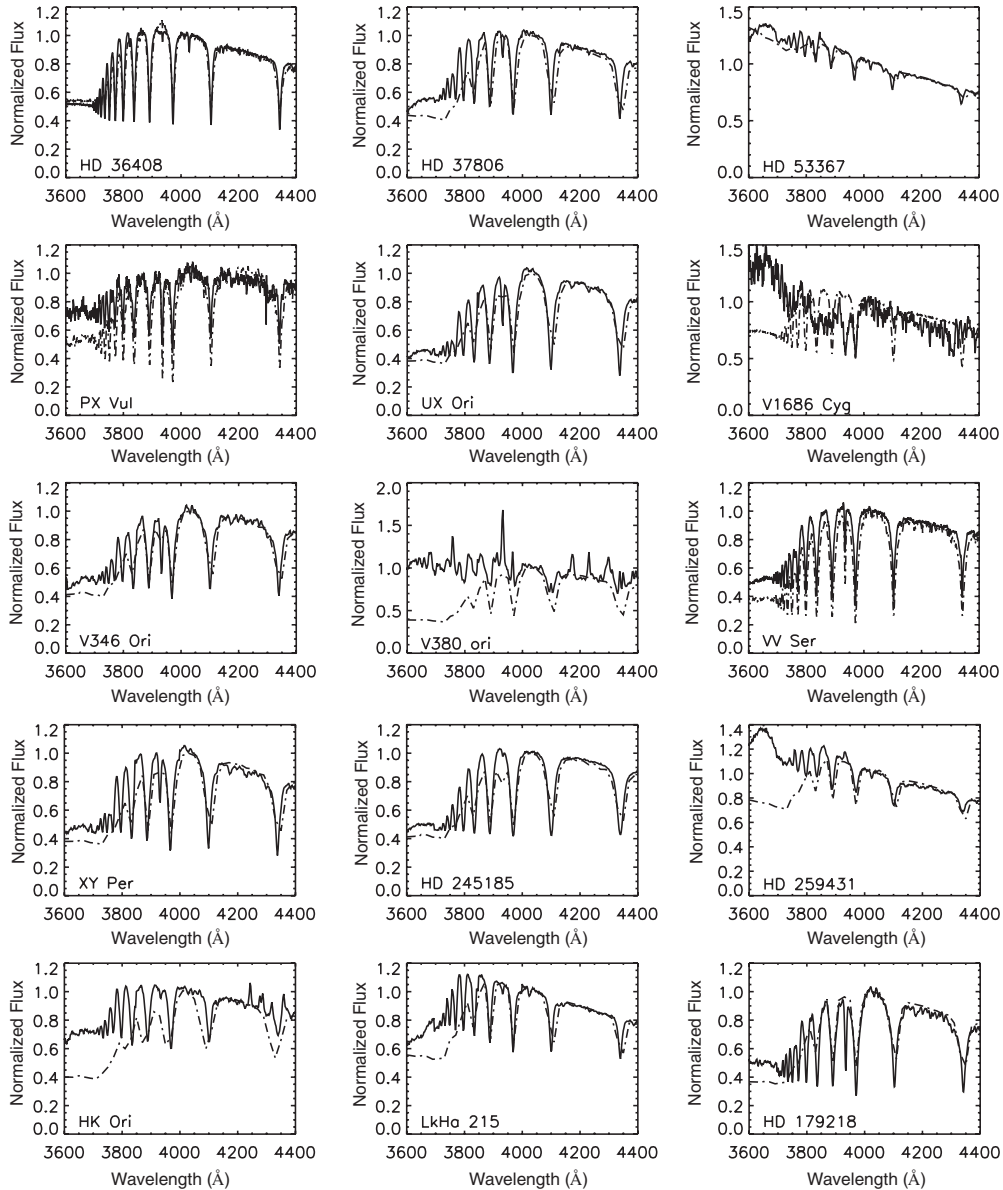
Figure 2. (Continued)

These differences may also be in part due to differences in methodology. However, over the period of our measurements, Br γ equivalent width, seems to show minimal variability. The variability that we do see would cause the Br γ luminosity to vary by a factor of two or less. This is consistent with the scatter that we see for our HAes. The variability is not large enough to explain the apparent lack of luminosity correlation for our HBe stars. Further, the luminosity of the Br γ line of HBes systematically overpredicts the accretion luminosity suggesting that the trend that holds for CTTS, IMTTS, and HAes does indeed breakdown for HBes.

Photospheric variability of our HAeBes could also contribute to the scatter seen in Figure 5. For our target stars, we use the Ks magnitude as measured by 2MASS. When we compare the 2MASS magnitudes of our stars to those found in Malfait et al. (1998), Hillenbrand et al. (1992), and Allen (1973), we find minimal variability (usually <10%) in the magnitude. However, Sitko et al. (2008) and Grady et al. (2010) found variability in HD 163296 and MWC 480, respectively. It may be that near contemporaneous observations of the Balmer discontinuity

and flux calibrated spectra of Br γ may shrink the scatter we observe in the relationship between the stellar accretion rate and luminosity of Br γ.

5. DISCUSSION

Our results show that the HAes in our sample have the same the Br γ/accretion luminosity relationship measured for CTTSs. The relationship for HAes holds down to an accretion rate of $10^{-8} M_{\odot}$ yr^{-1}. It is difficult to detect the accretion signature by observation of the Balmer discontinuity for lower rates (Muzerolle et al. 2004), thus the calibration of the luminosity of Br γ is uncertain for lower rates. The HBes have a Br γ luminosity that is systematically larger than predicted by the relationship presented by MHC98. This may indicate that the HBe stars have a source of hydrogen emission in addition to any purported accretion shock such as hydrogen recombination in the stellar wind. It is also possible that we are seeing the transition from magnetospheric accretion in the later sample to boundary layer accretion among the earlier type stars in the sample.

Table 3
Herbig Ae/Be Balmer Break Observations

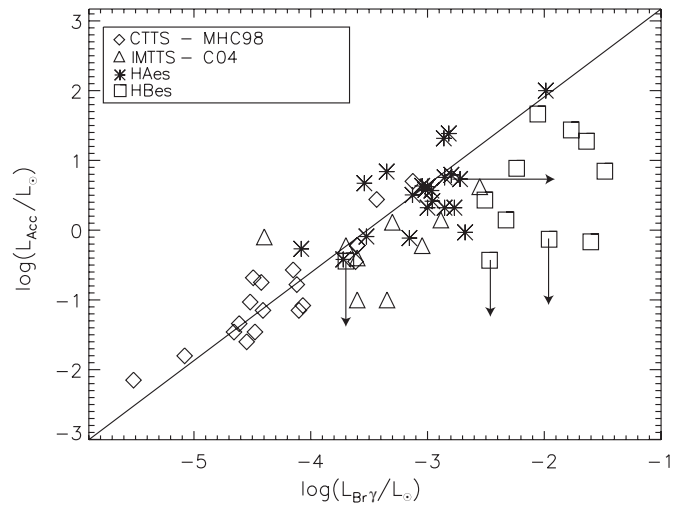| Star	ΔD_B	$\dot{M}$ ($10^{-7}\ M_\odot\ \text{year}^{-1}$)	L_{acc} ($L_\odot$)	Date of Observation
AB Aur	0.13	0.18 ± 0.04	0.67 ± 0.18	2009 Mar 19
BF Ori	0.22	0.87 ± 0.55	2.9 ± 2.0	2008 Mar 15
CQ Tau	0.26	1.12 ± 0.55	3.8 ± 2.0	2008 Mar 14
HD 142666	0.12	0.17 ± 0.04	0.38 ± 0.09	2009 Mar 19
HD 144432	0.13	0.18 ± 0.04	0.77 ± 0.18	2009 Mar 19
HD 163296	0.19	0.69 ± 0.41	2.1 ± 1.2	2009 Mar 21
HD 179218	0.33	1.90 ± 0.8	6.8 ± 2.8	2009 Mar 19
HD 244314	0.28	1.26 ± 0.55	3.8 ± 2.0	2009 Mar 19
HD 244604	0.18	0.63 ± 0.41	2.1 ± 1.2	2009 Mar 19
HD 245185	0.18	0.63 ± 0.41	2.6 ± 1.7	2008 Mar 13
HD 249879	<0.07	<0.1	<0.37	2008 Mar 15
HD 250550	0.11	0.16 ± 0.04	0.68 ± 0.17	2008 Mar 14
HD 259431	0.63	7.8 ± 0.5	46.2 ± 3	2008 Mar 13
HD 278937	0.40	2.2 ± 0.9	6.9 ± 2.8	2009 Mar 19
HD 35187	0.15	0.25 ± 0.2	0.81 ± 0.65	2008 Mar 13
HD 36112	0.67	8.9 ± 0.5	24.3 ± 1.5	2009 Mar 20
HD 36408	<0.04	<0.1	<0.36	2009 Mar 21
HD 37806	0.29	1.4 ± 0.5	5.4 ± 2.7	2008 Mar 16
HD 38120	0.28	1.26 ± 0.55	2.7 ± 1.6	2009 Mar 19
HD 50138	0.53	5.5 ± 0.4	18.8 ± 1.4	2009 Mar 19
HD 53367	<0.09	<0.12	<0.74	2008 Mar 14
HK Ori	0.67	5.6 ± 1	21 ± 2.0	2008 Mar 13
Lk Hα 215	0.34	1.9 ± 0.8	7.7 ± 3.2	2008 Mar 13
MWC 480	0.26	1.26 ± 0.55	4.2 ± 1.7	2008 Mar 15
PX Vul	0.35	1.9 ± 0.8	6.2 ± 2.6	2009 Mar 20
UX Ori	0.21	0.66 ± 0.43	2.1 ± 1.2	2008 Mar 15
V1686 Cyg	0.63	7.7 ± 0.54	27.3 ± 1.9	2009 Mar 22
V346 Ori	0.26	1.26 ± 0.55	4.7 ± 2	2008 Mar 13
V350 Ori	0.28	1.26 ± 0.55	4.3 ± 2	2009 Mar 19
V380 Ori	1.00	25 ± 1	100 ± 4	2008 Mar 14
VV Ser	0.16	0.32 ± 0.25	1.4 ± 1.1	2009 Mar 19
XY Per	0.25	0.95 ± 0.44	3.7 ± 1.9	2008 Mar 14
Z CMa	0.33	1.9 ± 0.8	7 ± 3	2008 Mar 14

Figure 3. Logarithm of the accretion luminosity vs. the logarithm of the Br γ luminosity. The HAe stars are represented by asterisks and the HBe stars are presented by squares. Data of classical T Tauri stars from Muzerolle et al. (1998) and intermediate-mass T Tauri stars from Calvet et al. (2004) are also plotted. These data are represented as diamonds and triangles, respectively. The best fit for classical T Tauri stars from Muzerolle et al. (1998) is plotted as a solid line.
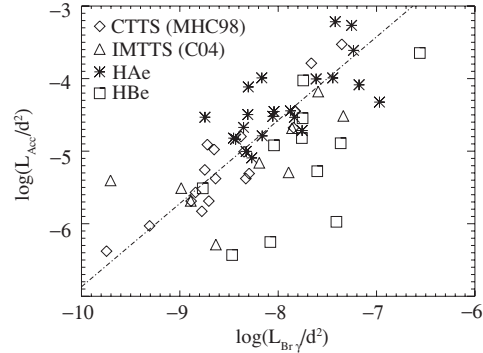

Figure 4. Logarithm of the accretion flux vs. the logarithm of the Br γ flux. The luminosity of Br γ and the accretion luminosity have been scaled by d^2 for the CTTSs (diamonds), IMTTSs (triangles), HAes (asterisks), and HBes (squares). The CTTSs, IMTTSs, and HAes follow the same trend indicating that the relationship is not driven by the d^2 dependence. The HBes do not follow the same trend. The flux of Br γ significantly overestimates the accretion flux.

Several studies point to important differences between HAes and HBes that are suggestive of such a transition. Measurement of the polarization of the Balmer lines H α, H β, and H γ suggest a divide between the origin of these lines in HAes and

Table 4
Herbig Ae/Be Br γ Variability

| Star	Spectral Type	EW (Obsv.) (Å) 2006 Nov	EW (Obsv.) (Å) 2007 Mar	EW (Obsv.) (Å) 2007 Sep	EW (Obsv.) (Å) 2008 Mar	GL06 (Å) 2004	BSNR07 (Å) 2002 Mar
HD 259431	B6	−5.4	. . .	. . .	−4.1	−6.68	. . .
HD 250550	B7	−4.8	. . .	. . .	−5.1	. . .	−6.38
VV Ser	B7	. . .	−3.7	. . .	−4.5	−9.0	. . .
HD 179218	B9	. . .	−1.0	. . .	. . .	1.3	. . .
HD 149914	B9	. . .	9.7	. . .	. . .	6.9	6.26
AB Aur	A0	. . .	. . .	−2.5	. . .	−4.4	−3.75
HD 163296	A1	. . .	. . .	. . .	−4.3	−4.7	−2.99
HD 150193	A1	. . .	−1.4	. . .	. . .	−3.5	. . .
HD 35187	A2	2.0	. . .	. . .	1.4	. . .	. . .
XY Per	A2	−0.8	. . .	−0.1	. . .	. . .	. . .
MWC 480	A3	−3.2	. . .	. . .	−4.0	. . .	. . .
HD 36112	A3	−3.7	. . .	. . .	−1.0	. . .	. . .
UX Ori	A3	−1.1	. . .	. . .	−0.7	−2.4	. . .
KK Oph	A8	−1.4	. . .	−1.4	−1.2	. . .	. . .
HD 142666	A8	. . .	1.9	1.8	2.1	1.02	. . .
HD 144432	A9	. . .	1.5	. . .	. . .	−2.1	. . .
HD 35929	F2	3.3	3.3	. . .	. . .	. . .	. . .
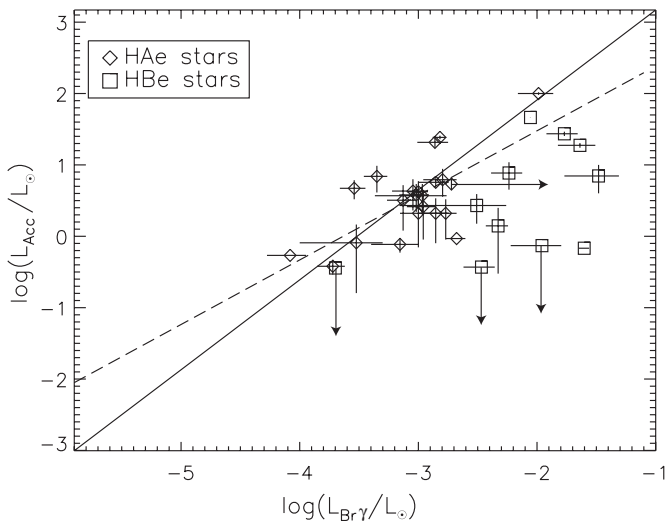
Figure 5. Logarithm of the accretion luminosity vs. the logarithm of the Br γ luminosity with error bars. The diamonds are HAe stars and the small squares are HBe stars. The dashed line is a weighted least-squares fit to the HAe stars while the solid line is the fit to CTTSs reported by MHC98.
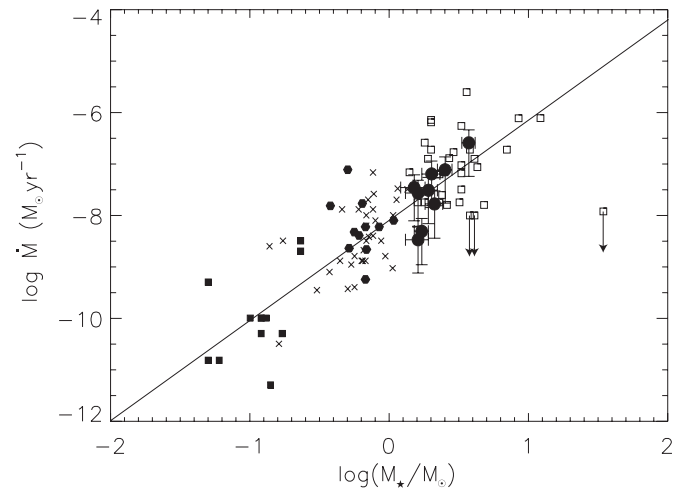

Figure 6. Logarithm of the stellar mass vs. the logarithm of the stellar accretion rate. We plot all of the HAeBe stars in our sample along with IMTTSs and CTTSs as plotted in C04. We used the accretion rate inferred from the veiling of the Balmer discontinuity for our data. Overplotted on the data is a line with a slope of 1.95 which was fit to the T Tauri stars by C04. We are not sensitive to accretion rates less than $10^{-8} M_{\odot}$ yr^{-1}. There is a scatter of about 2 dex which is comparable to that of the T Tauri stars.

HBes (Vink et al. 2002, 2005; Mottram et al. 2007). These authors note that the emission line is polarized in the case of the HAes, whereas the continuum is polarized and the emission line depolarized in the case of the HBes. They argue that the difference between the polarization effects in HAes and HBes is due to different disk geometries. In the case of the HAes, the line emission must originate interior to the disk as is expected if the line originates in a funnel-flow connecting the truncated disk to the star. In the case of the HBes, they note that the emission must be extended relative to the continuum. Further evidence of divide between HAes and HBes comes from radio observations. Skinner et al. (1993) note that they do not detect 3.6 cm radio emission from HAes of spectral type A2 or later and note that this similar to the case for Ap/Bp stars. They suggest that this is due to a sharp drop in the mass loss rate from hotter HBes to cooler HAes. If the correlation between the luminosity of Br γ and the accretion luminosity breaks down for earlier type HAeBes due to the increasing stellar wind, one might expect a gradual turnover as one moves from later HAes to earlier HBes. On the other hand, if the correlation breaks down because of a transition from magnetospheric accretion to a boundary layer accretion, one might expect a sharp discontinuity at the cut off. A larger sample of sources in the crucial A2–B7 range will help clarify how sharply this trend breaks down and is the subject of ongoing investigation.

Additional insight will be gained by further interferometric and spectro-astrometric observations of Br γ. Present studies have produced mixed results thus far (Kraus et al. 2008; Eisner et al. 2009); however, a survey of stars spanning spectral types A2–B7 may clarify why the trend between the luminosity of Br γ and the stellar accretion rate breaks down. Based on our results, it is possible, even likely, that the location of Br γ emission changes as the spectral types of the HAeBes move from A to B. For HAe stars, the emission may be tied to accretion, but for HBe stars the luminosity of Br γ may be dominated by emission from recombination in a stellar wind. If this is the case, then the spatial extent of the Br γ emission line will grow more extended for earlier type stars.

The physical explanation for the correlation between mass accretion rate and Br γ luminosity has yet to be resolved in

the case of HAes. However, its similarity with CTTSs provides some evidence that the accretion process is the same. If it is tied to magnetospheric-accretion, then HAe stars may be more magnetically active than hitherto expected. The conventional methods for detecting stellar magnetic fields, either through Zeeman broadening of spectral lines or the circular polarization of light from longitudinal field lines, fail to detect magnetic fields for most HAeBes (Hubrig et al. 2007; Wade et al. 2007). Skinner et al. (1993) place an upper limit on the magnetic field of HAeBe stars of 10kG based on the non-detection of a non-thermal radio signal from these sources. This is substantially stronger than the $\sim$2.5 kG fields observed for CTTSs (Johns-Krull 2007). It may be that the magnetic fields of HAe have an unusual topology, and may not have a strong dipole component. However, the line profile of emission from the CO molecule in the accretion disk can be used to trace the truncation radius of the disk. If the magnetic field truncates the gas at some radius above the stellar surface, it may be possible to extract the strength of the magnetic field by relating the truncation radius of the disk to the accretion rate of the star.

The stellar accretion rate of IMTTSs is proportional to $M_{\star}^{1.95}$ (C04). In Figure 6, we present the logarithm of the mass accretion rate as inferred from the veiling of the Balmer discontinuity versus stellar mass. We find that the trend observed for CTTSs and IMTTSs continues up to $12 M_{\odot}$. This is quite surprising as IMTTS are the evolutionary precursors to HAeBe stars. Thus one might expect that the accretion rate should be systematically lower for the HAeBes. It is conceivable that the evolution from the IMTTS state to the HAeBe state is fast enough that there is no significant difference between the accretion rate of HAeBes and IMTTSs on average. Further, there is no analog to weak-lined T Tauri stars among HAeBes. HAeBes are selected on the basis of evidence of circumstellar material, so it may be that HAeBes are a subset of the IMTTSs that tended to have more massive disks. It is also possible that the continuation of the trend we observe is due to our inability to detect accretion rates less than $10^{-8} M_{\odot}$ yr^{-1}. Further sampling of sources at the high end of our mass range may allow us to clarify whether this correlation breaks down.

6. CONCLUSION

We find that the luminosity of the Br γ emission from HAes correlates with the accretion luminosity in a manner similar to the correlation found for CTTS and IMTTS (MHC98; C04) for rates greater than $10^{-8}\,M_\odot\ \mathrm{yr}^{-1}$. The relationship breaks down for HBes. More observations of early HAes and late HBes should clarify the spectral type range over which the correlation becomes invalid and the manner in which it does so. It may be possible to improve the measurement of the correlation between the luminosity of Br γ and the stellar accretion rate with near contemporaneous observations of the Br γ line and Balmer discontinuity. This may be particularly important for clarifying how this correlation breaks down as one moves from HAes to HBes.

REFERENCES

Alecian, E., et al. 2007, in SF2A-2007: Proc. Annual Meeting of the French Society of Astronomy and Astrophysics Grenoble, France, 2007 July 2–6, ed. J. Bouvier, A. Chalabaev, & C. Charbonnel, 431
Allen, D. A. 1973, MNRAS, 161, 145
Ardila, D. R., Basri, G., Walter, F. M., Valenti, J. A., & Johns-Krull, C. M. 2002, ApJ, 567, 1013
Blondel, P. F. C., & Djie, H. R. E. T. A. 2006, A&A, 456, 1045
Bouvier, J., Alencar, S. H. P., Harries, T. J., Johns-Krull, C. M., & Romanova, M. M. 2007, in Protostars and Planets V, ed. B. Reipurth, D. Jewitt, & K. Keil (Tucson, AZ: Univ. Arizona Press), 479
Brittain, S. D., Najita, J. R., & Carr, J. S. 2009, ApJ, 702, 85
Brittain, S. D., Simon, T., Najita, J. R., & Rettig, T. W. 2007, ApJ, 659, 685
Calvet, N., & Gullbring, E. 1998, ApJ, 509, 802
Calvet, N., Muzerolle, J., Briceño, C., Hernández, J., Hartmann, L., Saucedo, J. L., & Gordon, K. D. 2004, AJ, 128, 1294 [C04]
D'Alessio, P., Calvet, N., & Hartmann, L. 2001, ApJ, 553, 321
D'Alessio, P., Calvet, N., Hartmann, L., Lizano, S., & Cantó, J. 1999, ApJ, 527, 893
Deleuil, M., Lecavelier des Etangs, A., Bouret, J.-C., Roberge, A., Vidal-Madjar, A., Martin, C., Feldman, P. D., & Ferlet, R. 2004, A&A, 418, 577

Eisner, J. A., Graham, J. R., Akeson, R. L., & Najita, J. 2009, ApJ, 692, 309
Feigelson, E. D., & Montmerle, T. 1999, ARA&A, 37, 363
Finkenzeller, U., & Mundt, R. 1984, A&AS, 55, 109
Garcia Lopez, R., Natta, A., Testi, L., & Habart, E. 2006, A&A, 459, 837
Garrison, L. M., Jr. 1978, ApJ, 224, 535
Grady, C. A., et al. 2010, ApJ, 719, 1565
Grinin, V. P., Kozlova, O. V., Natta, A., Ilyin, I., Tuominen, I., Rostopchina, A. N., & Shakhovskoy, D. N. 2001, A&A, 379, 482
Guimarães, M. M., Alencar, S. H. P., Corradi, W. J. B., & Vieira, S. L. A. 2006, A&A, 457, 581
Gullbring, E., Calvet, N., Muzerolle, J., & Hartmann, L. 2000, ApJ, 544, 927
Gullbring, E., Hartmann, L., Briceno, C., & Calvet, N. 1998, ApJ, 492, 323
Herbig, G. H. 1960, ApJS, 4, 337
Hillenbrand, L. A., Strom, S. E., Vrba, F. J., & Keene, J. 1992, ApJ, 397, 613
Hubrig, S., Pogodin, M. A., Yudin, R. V., Schöller, M., & Schnerr, R. S. 2007, A&A, 463, 1039
Johns-Krull, C. M. 2007, ApJ, 664, 975
Kraus, S., et al. 2008, A&A, 489, 1157
Malfait, K., Bogaert, E., & Waelkens, C. 1998, A&A, 331, 211
Manoj, P., Bhatt, H. C., Maheswar, G., & Muneer, S. 2006, ApJ, 653, 657
Montesinos, B., Eiroa, C., Mora, A., & Merín, B. 2009, A&A, 495, 901
Mottram, J. C., Vink, J. S., Oudmaijer, R. D., & Patel, M. 2007, MNRAS, 377, 1363
Muzerolle, J., Calvet, N., & Hartmann, L. 2001, ApJ, 550, 944
Muzerolle, J., D'Alessio, P., Calvet, N., & Hartmann, L. 2004, ApJ, 617, 406
Muzerolle, J., Hartmann, L., & Calvet, N. 1998, AJ, 116, 2965 [MHC98]
Najita, J., Carr, J. S., & Mathieu, R. D. 2003, ApJ, 589, 931
Natta, A., Grinin, V. P., & Tambovtseva, L. V. 2000, ApJ, 542, 421
Palla, F., & Stahler, S. W. 1993, ApJ, 418, 414
Reed, B. C. 2003, AJ, 125, 2531
Schiavon, R. P., Batalha, C., & Barbuy, B. 1995, A&A, 301, 840
Sitko, M. L., et al. 2008, ApJ, 678, 1070
Skinner, S. L., Brown, A., & Stewart, R. T. 1993, ApJS, 87, 217
Skinner, S. L., & Yamauchi, S. 1996, ApJ, 471, 987
Stelzer, B., Micela, G., Hamaguchi, K., & Schmitt, J. H. M. M. 2006, A&A, 457, 223
Strom, S. E., Strom, K. M., Yost, J., Carrasco, L., & Grasdalen, G. 1972, ApJ, 173, 353
The, P. S., de Winter, D., & Perez, M. R. 1994, A&AS, 104, 315
Tout, C. A., & Pringle, J. E. 1995, MNRAS, 272, 528
Tout, C. A., & Pringle, J. E. 1996, MNRAS, 281, 219
Valenti, J. A., Basri, G., & Johns, C. M. 1993, AJ, 106, 2024
Valenti, J. A., & Johns-Krull, C. M. 2004, Ap&SS, 292, 619
van den Ancker, M. 2005, in Proc. ESO Workshop on High Resolution Infrared Spectroscopy in Astronomy, Garching, Germany, 2003 November 18–21, ed. H.U. Käufl, R. Siebenmorgen, & A. Moorwood, 309
van den Ancker, M. E., de Winter, D., & Tjin A Djie, H. R. E. 1998, A&A, 330, 145
Vieira, S. L. A., Corradi, W. J. B., Alencar, S. H. P., Mendes, L. T. S., Torres, C. A. O., Quast, G. R., Guimarães, M. M., & da Silva, L. 2003, AJ, 126, 2971
Vink, J. S., Drew, J. E., Harries, T. J., & Oudmaijer, R. D. 2002, MNRAS, 337, 356
Vink, J. S., Harries, T. J., & Drew, J. E. 2005, A&A, 430, 213
Wade, G. A., Bagnulo, S., Drouin, D., Landstreet, J. D., & Monin, D. 2007, MNRAS, 376, 1145
Wallace, L., & Hinkle, K. 1998, VizieR Online Data Catalog, 211, 10445